

Task 4. Cloth Rendering

Garoe Dorta-Perez

CM50245: Computer Animation and Games II

May 27, 2015

1 Introduction

Rendering realistic images is a challenging task, specially if there are memory or time constraints for the computation. Cloth is a complex material composed of interwoven threads of different types. Moreover, its appearance can vary from diffuse to highly specular.

2 Previous work

Solving for global illumination generally involves providing a solution to the rendering equation [5]. One of the earliest approaches was based on simple empirical shading models [16]. The main objective was to accomplish believable shading, disregarding physical accuracy. Ever since, an increasing number of methods have been proposed, this techniques can be broadly divided into two groups, data-based models and procedural models.

The data-based approach focuses on collecting reflectance information, that will be later used to model the cloth. Bidirectional Texture Function (BTF) [2] is a function that is often used to sampled in the data based techniques. [10] captured BTF from a rectangular probed and generated view-dependant texture-maps for the cloth. Wang et al. [14] proposed a variation of the previous technique, the authors modeled the captured data as a microfacet-based BRDF to which they fitted a normal distribution function for each facet. Within the data-based models, a volumetric method was proposed by Zhao et al. [18]. The authors capture a X-ray computed tomography (CT) scanner of the fabric, which is later matched to images of the same material.

Geometric models focus on simulation the micro-geometry of the cloth in conjunction with global illumination. The light scattering is simulated for each fibre in the thread, where the fibres are modelled as perfect cylinders. To be able to model the the complete scattering effects on a surface, Bidirectional Scattering-Surface Reflectance Distribution Function (BSSRDF) [8] have been used. With this function, complex light phenomena like subsurface scattering are modelled.

Procedural models [3] with enfasis on accurately handling specular reflections have been proposed, this model does not required image data and relies on textures for close up views.

A survey of physically-based methods in cloth simulations was presented by Schröder et al. [12], we also refer the readers to Yuen and Wünsche’s [17] survey for example-based and procedural-based techniques.

3 Methodology

In this section we will discuss in detail the theoretical and practical aspects of the chosen paper.

3.1 Light scattering model

We have chosen to implement a recent paper [9] which presents a microcylinder based model for fast and realistic cloth rendering. The authors propose a model of fabric based on two microcylinders oriented in two orthogonal directions, as shown in Figure 1. Sadeghi et al. define the reflectance model for a single thread in the fabric as

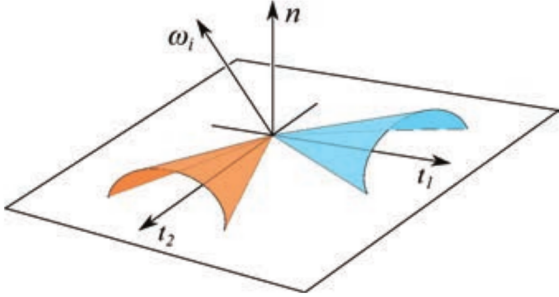


Figure 1: Sadeghi et al. shading model [9], where ω_i is the incident light direction, \mathbf{n} is the surface normal and $\mathbf{t}_1, \mathbf{t}_2$ are the orthogonal thread directions.

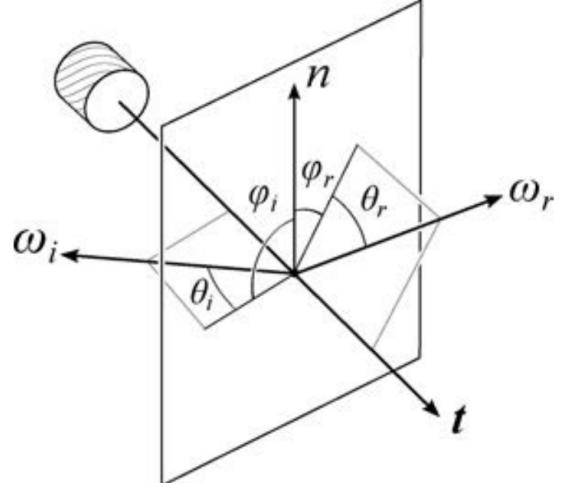


Figure 2: Sadeghi et al. shading model [9], showing θ and ϕ angles given a pair of directions ω_i and ω_r .

$$L_r = \int \frac{(f_{r,s}(\mathbf{t}, \omega_i, \omega_r) + f_{r,v}(\mathbf{t}, \omega_i, \omega_r)) L_i(\omega_i) \cos(\theta_i) \delta\omega_i}{\cos^2(\theta_d)}, \quad (1)$$

where \mathbf{t} is the thread direction, ω_i is the ray incoming direction, ω_r is the ray outgoing direction, θ_i , θ_r , ϕ_i and ϕ_r are angles as shown in Figure 2, $\theta_d = \theta_i - \theta_r$ and L_i is the incoming irradiance in the evaluated point. Note that radiometric notation [6] is used to define L_r , which represents the outgoing radiance over a infinitesimal arc length of the cylinder and how the integral extends over the entire sphere instead of the typical hemisphere.

The surface reflection term in Equation 1 is defined as

$$f_{r,s}(\mathbf{t}, \omega_i, \omega_r) = F_r(\eta, \omega_i) \cos(\phi_d/2) g(\gamma_s, \theta_h), \quad (2)$$

where $\theta_h = (\theta_i + \theta_r)/2$, $\phi_d = \phi_i - \phi_r$, F_r is a Fresnel reflection term that is computed using Schlick's approximation [11] $F_r(\eta, \boldsymbol{\omega}_i) = \eta + (1 - \eta)(1 - \mathbf{h} \cdot \boldsymbol{\omega}_i)^5$ where \cdot is the vector dot product operator, $\mathbf{h} = (\boldsymbol{\omega}_i + \boldsymbol{\omega}_r)/|\boldsymbol{\omega}_i + \boldsymbol{\omega}_r|$ is the normalized halfway vector, η is the reflectance for $\mathbf{h} \cdot \boldsymbol{\omega}_i = 1$, $g(\gamma, \theta) = \gamma e^{\mathbf{j} \cdot \mathbf{q} - 1}$ is a Gaussian lobe [15] where \mathbf{q} is the lobe axis, the direction \mathbf{j} is the spherical parameter in the resulting function and γ is the amplitude.

The volume scattering term in Equation 1 is defined as

$$f_{r,v}(\mathbf{t}, \boldsymbol{\omega}_i, \boldsymbol{\omega}_r) = F_t(\eta, \boldsymbol{\omega}_i) F_t(\eta', \boldsymbol{\omega}'_r) \frac{(1 - k_d)g(\gamma_v, \theta_h) + k_d \mathbf{k}_a}{\cos(\theta_i) + \cos(\theta_r)}, \quad (3)$$

where k_d is a scattering constant, \mathbf{k}_a is an rgb albedo constant vector, $F_t = 1 - F_r$ is a Fresnel transmission term, $\boldsymbol{\omega}'_r$ is a projection of $\boldsymbol{\omega}_r$ into a plane that contains the normal \mathbf{n} and η' is computed using the Bravais index [6] as $\eta'(m) = \sqrt{\eta^2 - \sin^2(m)}/\cos(m)$ where m is the angle between $\boldsymbol{\omega}_r$ and its projection $\boldsymbol{\omega}'_r$.

The outgoing radiance in the path shown in Figure 2 is

$$L_r(\boldsymbol{\omega}_r) = a_1 L_{r,1}(\boldsymbol{\omega}_r) + a_2 L_{r,2}(\boldsymbol{\omega}_r), \quad (4)$$

where a_1 and a_2 are the area coverage ratio for the first and second thread within the patch, in our case we assume a watertight pattern of equally size threads, leading to $a_1 = a_2 = 0.5$, L_1 and L_2 are the outgoing radiances for the first and second thread computed as shown in Equation 1.

In order to compute a thread direction \mathbf{t} without using external data structures, we follow a fixed texture axis as shown in Figure 3. Given an intersection point in a triangle $\mathbf{p} = [x_p, y_p, z_p]$ and its texture coordinates $\mathbf{u} = [u_p, v_p]$. We define \mathbf{t} vector as the vector $\mathbf{t} = (\hat{\mathbf{p}} - \mathbf{p})/|\hat{\mathbf{p}} - \mathbf{p}|$ such that $\hat{\mathbf{p}}$ texture coordinates are $\hat{\mathbf{u}} = [u_p + 1, v_p]$. In our shader we can easily compute the texture coordinates of the triangle vertices, however we can not immediately get a world position from a new texture coordinate. Assuming that the 3d to texture transformation is an affine matrix T ,

$$\mathbf{u}T = \mathbf{p} \rightarrow \begin{pmatrix} u & v \end{pmatrix} \begin{pmatrix} a_{11} & a_{12} & a_{13} \\ a_{21} & a_{22} & a_{23} \end{pmatrix} = \begin{pmatrix} x & y & z \end{pmatrix} \quad (5)$$

The system in Equation 5 has six unknowns and three equations, therefore we need two pairs of world points - texture coordinates to solve T . Writing out the terms for two known points \mathbf{p}_1 and \mathbf{p}_2 in the triangle,

$$\begin{aligned} x_1 &= u_1 a_{11} + v_1 a_{21}, & y_1 &= u_1 a_{12} + v_1 a_{22}, & z_1 &= u_1 a_{13} + v_1 a_{23}, \\ x_2 &= u_2 a_{11} + v_2 a_{21}, & y_2 &= u_2 a_{12} + v_2 a_{22}, & z_2 &= u_2 a_{13} + v_2 a_{23}. \end{aligned} \quad (6)$$

Solving for each term analytically,

$$a_{21} = \frac{u_2 x_1 - u_1 x_2}{u_2 v_1 - u_1 v_2}, \quad a_{22} = \frac{u_2 y_1 - u_1 y_2}{u_2 v_1 - u_1 v_2}, \quad a_{23} = \frac{u_2 z_1 - u_1 z_2}{u_2 v_1 - u_1 v_2}, \quad (7)$$

$$a_{11} = \frac{x_1 - v_1 a_{21}}{u_1}, \quad a_{12} = \frac{y_1 - v_1 a_{22}}{u_1}, \quad a_{13} = \frac{z_1 - v_1 a_{23}}{u_1}. \quad (8)$$

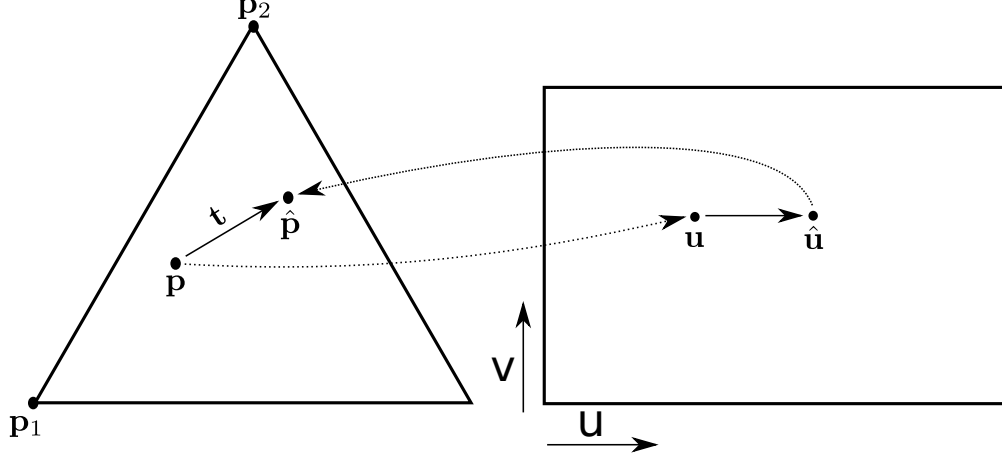


Figure 3: To compute the vector \mathbf{t} , we follow the texture coordinates of the intersection point \mathbf{p} .

Notice that the term of $1/(u_2v_1 - u_1v_2)$ is shared, so it can be precomputed in order to increase performance. The aforementioned method will give \mathbf{t}_1 , for \mathbf{t}_2 the process is equivalent with the exception that $\hat{\mathbf{u}}$ will be incremented on the v direction, $\hat{\mathbf{u}} = [u_p, v_p + 1]$.

3.2 Shading model

In order to render cloth fabrics the authors evaluate the outgoing radiance from each patch, which is assumed to be locally flat and smaller than a pixel in the image. This patch is defined as the smallest thread weaving pattern such that the fabric can be constructed by repeating this patch, as shown in Figure 4. For each thread in the patch a tangent curved is defined, this curve will be sampled at fixed positions giving the normal direction in that position, as shown in Figure 4. The BRDF will be evaluated for each sample and the total outgoing radiance will be computed as follows,

$$L_r(\omega_r) = \frac{1}{N_j} \sum_{\mathbf{t}} \int L_i(\omega_i) f_s(\mathbf{t}, \omega_i, \omega_r) \cos \theta_i d\omega_i, \quad (9)$$

where N_j is the number of samples.

Sadeghi et al. also add a shadowing and masking term to improve the quality of their results, the authors add a new term that will account for threads occluding each other depending on the viewing direction. The effect of the masking term will be specially relevant at grazing angle viewing and lighting directions. In Equation 9 the term $f_s(\mathbf{t}, \omega_i, \omega_r)$ will be multiplied by $M(\mathbf{t}, \omega_i, \omega_r)$ such that,

$$M(\mathbf{t}, \omega_i, \omega_r) = (1 - u(\phi_d)) \max(\cos(\phi_i), 0) \times \max(\cos(\phi_r), 0) + u(\phi_d) \min(\max(\cos(\phi_i), 0), \max(\cos(\phi_r), 0)), \quad (10)$$

where \times is the vector cross product operator, u is a unit height Gaussian function with standard deviation between 15° and 25° ; an in depth discussion on how to compute u can be found in Ashikmin et al. [1] Section 4.2 New Shadowing Term.

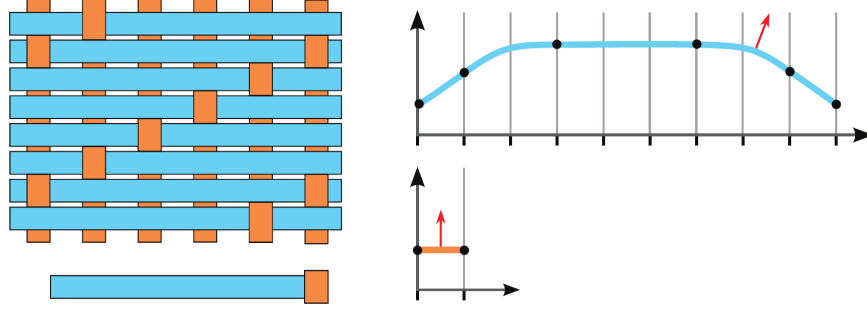


Figure 4: Weaving pattern and tangent curves: (top left) a weaving pattern example, (bottom left) the smallest patch, (top right) tangent curve for the blue thread in the smallest patch, (bottom right) tangent curve for the orange thread in the smallest patch, arrows indicate a normal sampled at that point, image taken from [9].

The authors add a reweighting factor to account for ω_i and ω_r being too far from n . By projecting the thread length in the direction of the viewer, tangents that are more visible for the viewer will have a greater contribution. The reweighting factor $P(\mathbf{t}, \omega_i, \omega_r)$ will be computed as follows,

$$P(\mathbf{t}, \omega_i, \omega_r) = (1 - u(\Psi_d)) \max(\cos(\Psi_i), 0) \times \max(\cos(\Psi_r), 0) + u(\Psi_d) \min(\max(\cos(\Psi_i), 0), \max(\cos(\Psi_r), 0)), \quad (11)$$

where Ψ are the angles between \mathbf{n} and the projection of ω into the plane that contains \mathbf{t} and \mathbf{n} , as shown in Figure 5.

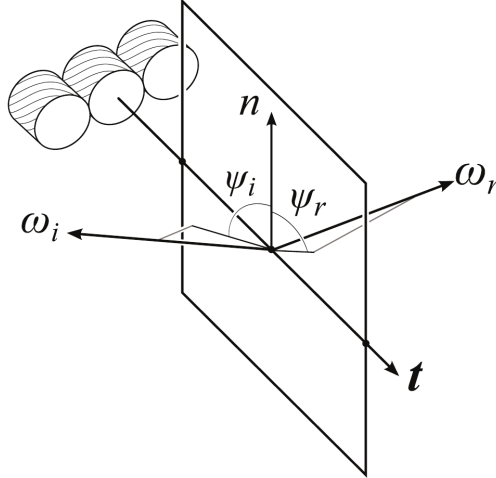


Figure 5: Ψ angles in the thread for a given ω_i and ω_r , image taken from [9].

There is also a normalization factor Q to account for the number of samples and for weaving patterns that are not water tight,

$$Q = \frac{a_1}{N_1} \sum_{\mathbf{t}} P(\mathbf{t}, \omega_i, \omega_r) + \sum_{\mathbf{t}} P(\mathbf{t}, \omega_i, \omega_r) + (1 - a_1 - a_2)(\omega_r \cdot \mathbf{n}), \quad (12)$$

where N_1 and N_2 are the number of samples of each thread direction. Finally, the complete model for the outgoing radiance is

$$L_r(\omega_r) = \frac{1}{QN_j} \sum_{\mathbf{t}} \int L_i(\omega_i) f_s(\mathbf{t}, \omega_i, \omega_r) M(\mathbf{t}, \omega_i, \omega_r) P(\mathbf{t}, \omega_i, \omega_r) \cos \theta_i d\omega_i. \quad (13)$$

3.3 Other implementation considerations

In order to compute more easily quantities such as the θ or ϕ angles introduced in the previous section, we will define a new coordinate system with the vectors $\{\mathbf{t}, \mathbf{n}, \mathbf{s}\}$, whose centre will be the triangle ray-intersection point \mathbf{p} , where \mathbf{s} is a normalized vector $\mathbf{s} = \mathbf{n} \times \mathbf{t}$. The matrix that will transform from world coordinates to this system is

$$M = M_{trans} M_{rot} = \begin{pmatrix} 1 & 0 & 0 & 0 \\ 0 & 1 & 0 & 0 \\ 0 & 0 & 1 & 0 \\ -p_x & -p_y & -p_z & 1 \end{pmatrix} \begin{pmatrix} t_x & n_x & s_x & 0 \\ t_y & n_y & s_y & 0 \\ t_z & n_z & s_z & 0 \\ 0 & 0 & 0 & 1 \end{pmatrix}, \quad (14)$$

such that $\mathbf{x}M = \mathbf{x}'_{new}$, where \mathbf{x} is the original row vector in homogeneous coordinates and \mathbf{x}'_{new} is the transformed vector.

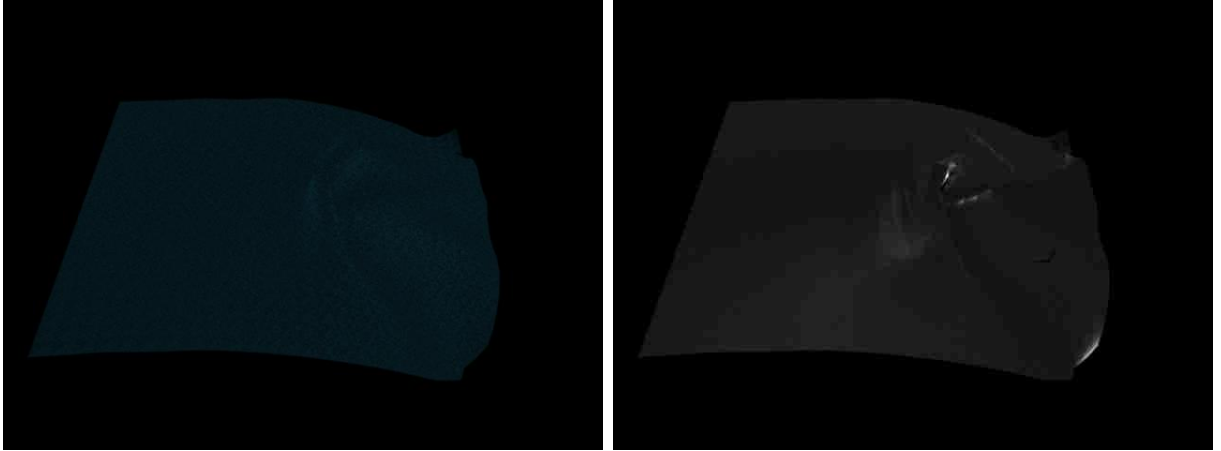
We decided to implement the shader in Maya's[®]Mental Ray[®]rendering software. The rationale under this choice lays in the advantages of integrating work in a established framework, which allows us to easily use the shader for a dynamic cloth simulation. Mental Ray[™] approximates Kajiya's equation [5] using photon mapping [4]. Our approach is to compute an initial estimate of the outgoing radiance L_{ri} for each direct hit during the raytracing path. In the photon map construction stage each photon hit will locally sample L_{ri} using Equation 1, from this samples an average irradiance will be evaluated, which will then be added to the initial estimate as shown below

$$L_r = L_{ri} + \sum_{i=1}^I \psi_i L_{ri}, \quad (15)$$

where I is the total number of photons inside a fixed radius around \mathbf{p} and ψ_i is the normalized flux of the i th photon, which is computed from an initial arbitrary flux shared by all photons and decreases with an absorption rate per bounce.

4 Results

We have implemented the basic light scattering model in Mental Ray[®]. To better understand the effects of the different terms in the BRDF, results for the different parts are evaluated separately. The cloth rendered using only the volume scattering term is shown in Figure 6a, using only the reflection term is shown in Figure 6b, note that for visualization purposes the reflection term has been increased by a factor of 5. Lastly, a rendered image for the fabric using both terms is shown in Figure 7.



(a) Effect of the volume scattering term.

(b) Effect of the reflection term, scaled by 2 to improve visibility.

Figure 6: Evaluating the effects of the different terms of the BRDF.

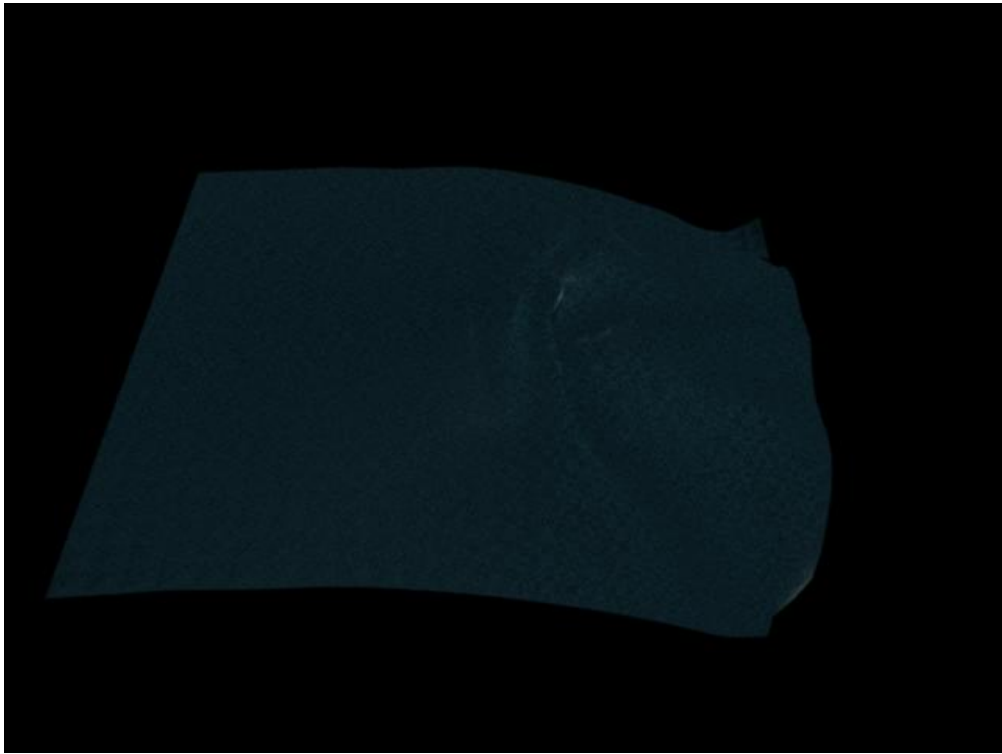


Figure 7: Final result.

5 Conclusion and Future Work

Our implementation only includes the basic light scattering proposed by the authors [9]; so a evident line of future work would be to add the remaining features from the paper into our code. Sadeghi et al. model works under the assumption that the cloth patches are smaller than a pixel in the image, this leads to incorrect render images at close ups. Another drawback of the model is the optimization of parameters, being so complex that they have to be adjusted manually. How to efficiently apply importance sampling to reduce the rendering times and increase quality, has been addressed with several extensions to the original paper [13, 7].

References

- [1] M Ashikmin, S Premože, and Peter Shirley. A Microfacet-based BRDF Generator. In *Proceedings of the 27th annual conference on Computer graphics and interactive techniques*, pages 65–74, 2000.
- [2] K.J. Dana, S.K. Nayar, B. Van Ginneken, and J.J. Koenderink. Reflectance and texture of real-world surfaces. *ACM Transactions on Graphics*, 18(1):1–34, 1999.
- [3] Piti Irawan and Steve Marschner. Specular reflection from woven cloth. *ACM Transactions on Graphics*, 31(1):1–20, 2012.
- [4] Henrik W. Jensen. Global illumination using photon maps. In *Rendering Techniques '96*, pages 21–30. Springer-Verlag, 1996.
- [5] James T. Kajiya. The rendering equation. *SIGGRAPH Computer Graphics*, 20(4):143–150, 1986.
- [6] Stephen R. Marschner, Henrik Wann Jensen, Mike Cammarano, Steve Worley, and Pat Hanrahan. Light scattering from human hair fibers. *ACM Transactions on Graphics*, 22(3):780–791, 2003.
- [7] Kazutaka Mizutani and Kei Iwasaki. Importance Sampling for Cloth Rendering under Environment Light. In *Mathematical Progress in Expressive Image Synthesis I*, pages 81–88. 2014.
- [8] Fred E. Nicodemus, Joseph C. Richmond, Jack J. Hsia, Irving W. Ginsberg, and Thomas Limperis. *Geometrical considerations and nomenclature for reflectance*. National Bureau of Standards Washington, DC, USA, 1977.
- [9] Iman Sadeghi, Oleg Bisker, Joachim de Deken, and Henrik Wann Jensen. A practical microcylinder appearance model for cloth rendering. *ACM Transactions on Graphics*, 32(2):1–12, 2013.
- [10] Mirko Sattler, Ralf Sarlette, and Reinhard Klein. Efficient and realistic visualization of cloth. In *Proceedings of the 14th Eurographics Workshop on Rendering*, EGRW '03, pages 167–177, 2003.
- [11] Christophe Schlick. An Inexpensive BRDF Model for Physically-based Rendering. In *Computer Graphics Forum*, volume 13, pages 233–246, 1994.
- [12] Kai Schröder, Shuang Zhao, and Arno Zinke. Recent Advances in Physically-Based Appearance Modeling of Cloth. In *SIGGRAPH Asia 2012 Courses*, pages 12:1–12:52, 2012.
- [13] Chunpo Wang, Feng Xie, and Parashar Krishnamachari. Importance Sampling for a Microcylinder Based Cloth BsdF. In *ACM SIGGRAPH 2014 Talks*, pages 41:1—41:1, 2014.

- [14] Jiaping Wang, Shuang Zhao, Xin Tong, John Snyder, and Baining Guo. Modeling anisotropic surface reflectance with example-based microfacet synthesis. *ACM Trans. Graph.*, 27(3):41:1–41:9, 2008.
- [15] Jiaping Wang, Peiran Ren, Minmin Gong, John Snyder, and Baining Guo. All-Frequency Rendering of Dynamic, Spatially-Varying Reflectance. *ACM Transactions on Graphics*, 28(5):133:1–133:10, 2009.
- [16] Jerry Weft and Murray Hill. The Synthesis of Cloth Objects. *SIGGRAPH Computer Graphics*, 20(4):49–54, 1986.
- [17] Wallace Yuen and B Wünsche. An evaluation on woven cloth rendering techniques. In *Proceedings of the 26th International Image and Vision Computing New Zealand Conference (IVCNZ 2011)*, pages 7–12, 2011.
- [18] Shuang Zhao, Wenzel Jakob, Steve Marschner, and Kavita Bala. Building volumetric appearance models of fabric using micro ct imaging. *ACM Trans. Graph.*, 30(4):44:1–44:10, 2011.